Available online at www.sciencedirect.com
SCIENCE DIRECT
Cement and Concrete Research 36 (2006) 1042–1047
Cement and Concrete Research

A porosimetric study of calcium sulfoaluminate cement pastes cured at early ages

Graziella Bernardo, Antonio Telesca, Gian Lorenzo Valenti *

Dipartimento di Ingegneria e Fisica dell'Ambiente, Facoltà di Ingegneria, Università degli Studi della Basilicata Via dell'Ateneo Lucano, 10, 85100 Potenza, Italy

Received 3 December 2004; accepted 21 February 2006

Abstract

Calcium sulfoaluminate and Portland cement pastes, both prepared with a water/solid mass ratio equal to 0.5 and cured for time periods comprised between 2 h and 28 days, show completely different pore size distributions by mercury intrusion. Portland cement pastes aged at 12 h and 1 day exhibit a unimodal distribution of pore sizes related to a continuous network of capillary pores with a threshold pore radius decreasing from nearly 650 to 350 nm. After 7 and 28 days of curing, this parameter shifts to about 150 nm and a region having smaller pores appears (with a second threshold pore radius roughly comprised between 10 and 30 nm), made discontinuous by blockages of hydration products which occlude the interconnected pore system and isolate the interior space. For calcium sulfoaluminate cement pastes, a bimodal distribution is rapidly established, in which the regions with a lower porosity (threshold pore radii up to about 25 nm) are dominant, while the decrease of total porosity almost ceases at later ages. The porosimetric behaviour of calcium sulfoaluminate-based cement is related to its very fast hydration rate and to the lack of water needed to continue the hydration reactions.

Keywords: Hydration; Characterization; Mercury porosimetry; Pore size distribution; Sulfoaluminate cement

1. Introduction

The most important property of $C_4A_3\overline{S}$-based cements has been considered for a long time the ability of their key component, when hydrated in the presence of calcium sulfate and calcium hydroxide, to generate expansive ettringite. Several calcium sulfoaluminate ($C\overline{S}A$) formulations, alone or mixed with Portland cement, are used as shrinkage-compensating or self-stressing binders [1–6]. However $C\overline{S}A$ cements show other interesting features such as, for example, the environment-friendly character of their manufacturing process [7–16]. In this regard, compared to Portland clinkers, $C\overline{S}A$ clinkers can be synthesized at lower temperatures (about 1250 °C) and, due to their higher porosity, are easier to grind. The limestone concentration in the raw mix is reduced and, consequently, kiln thermal requirements and CO_2 generation are decreased per unit mass of clinker. Moreover, a large number of industrial wastes and by-products, whose disposal or reuse is sometimes quite complicated, can be successfully used for the manufacture of $C\overline{S}A$ cements [12–16].

During the last decade, the interest of several researchers and engineers has been attracted by rapid-hardening and dimensionally stable $C\overline{S}A$ cements, containing also dicalcium silicate and calcium aluminates, developed by the China Building Materials Academy [4,17–20]. $C_4A_3\overline{S}$ reacts with calcium sulfate (normally added but also present in the clinkers) and water to give a non-expansive ettringite which achieves high mechanical strength at early ages. Moreover, well-made matrices have high freeze–thaw and chemical resistance, low values of dry shrinkage, permeability and solution alkalinity (but not such a low alkalinity that embedded steel is depassivated). The remarkable properties of Chinese $C\overline{S}A$ formulations are useful for a variety of special applications. New uses have been recently suggested [21,22]. In recent years, papers concerning both the study of the hydration chemistry of $C\overline{S}A$ cements and the interpretation of their engineering properties have been published [23–26].

* Corresponding author.
E-mail address: valenti@unibas.it (G.L. Valenti).

0008-8846/$ - see front matter © 2006 Elsevier Ltd. All rights reserved.
doi:10.1016/j.cemconres.2006.02.014

Porosity development in hydrated cements generally plays an important role in regulating their technical behaviour. This is particularly true for hydrated $C\bar{S}A$ cements inasmuch as the amount of chemically bound water is much higher than that of hydrated Portland cements [19,27,28]: due to the reduction of available free water, $C\bar{S}A$ cements are expected to have a different evolution of porosity.

The aim of this paper is to investigate, by mercury intrusion porosimetry, the development of the pore structure of a rapid-hardening $C\bar{S}A$ cement hydrated at early ages, using Portland cement as a reference matrix.

2. Experimental

2.1. Materials

2.1.1. Calcium sulfoaluminate cement

The rapid-hardening $C\bar{S}A$ cement was obtained from a sulfoaluminate clinker synthesized in a pilot rotary kiln at 1300 °C. Its Blaine fineness was 0.500 m^2/g.

The cement composition in terms of the major oxides is reported in Table 1 and the crystalline phases identified by X-ray diffraction analysis were $C_4A_3\bar{S}$, $C\bar{S}$, α'-C_2S and $C_{12}A_7$ whose estimated concentration values are 53.0, 18.6, 13.2 and 10.3 mass%, respectively.

Table 2 shows the mortar compressive strength at 3 h, 8 h, 1 day, 2 days, 7 days and 28 days (sand/cement/water mass ratios equal to 3:1:0.5, respectively).

2.1.2. Portland cement

A II-A/L class 42.5 R Portland limestone cement, containing 12% of limestone and 4.5% of natural gypsum, was also investigated. Its Blaine fineness was 0.460 m^2/g. The chemical composition and the compressive strength results on mortar (3:1:0.5) are illustrated in Tables 1 and 2, respectively.

2.2. Characterization techniques

2.2.1. Mercury intrusion porosimetry

The porosity measurements were performed using a Thermo Finnigan Pascal 240 Series porosimeter (maximum pressure, 200 MPa) equipped with a low-pressure unit (140 Series) able to generate a high vacuum level (10 Pa) and operate between 100 and 400 kPa. Samples of both cements, paste hydrated (w/c = 0.5) and shaped as cylindrical discs (15 mm high, 30 mm in diameter), were cured for times ranging between 2 h and 28 days. Before the test, at the end of each aging period, the samples were broken, treated with acetone and diethyl-ether to stop hydration and stored in a desiccator over silica gel–soda lime ensuring protection against water and carbon dioxide. Residual gases and vapours were evacuated in the porosimetric low-pressure unit. For each sample, two plots can be obtained from the porosimetric analysis: (a) cumulative and (b) derivative Hg intruded volume vs. pore radius.

With increasing pressure, mercury gradually penetrates the bulk sample volume. If the pore system is composed by an interconnected network of capillary pores in communication with the outside of the sample, mercury enters at a pressure value corresponding to the smallest pore neck. If the pore system is discontinuous, mercury may penetrate the sample volume if its pressure is sufficient to break through pore walls. In any case, the pore width related to the highest rate of mercury intrusion per change in pressure is known as the "critical" or "threshold" pore width [29]. Unimodal, bimodal or multimodal distribution of pore sizes can be obtained, depending on the occurrence of one, two or more peaks, respectively, in the derivative volume plot.

Table 1
Chemical composition of sulfoaluminate and Portland cements, mass%

	Sulfoaluminate	Portland
CaO	41.4	62.0
Al_2O_3	27.6	4.8
SiO_2	5.1	17.1
Fe_2O_3	1.5	2.4
SO_3	22.3	3.1
MgO	1.0	2.2
Loss on ignition	–	5.3
Total	98.9	96.9

Table 2
Mortar compressive strength of sulfoaluminate and Portland cements, MPa [a]

	3 h	8 h	1 day	2 days	7 days	28 days
Sulfoaluminate	24.0	38.9	59.1	67.5	68.5	68.7
Portland	–	2.0	20.2	29.1	41.3	46.1

[a] According to EN 196-1 Standard.

2.2.2. X-ray diffraction and differential thermal–thermogravimetric analyses

X-ray diffraction (XRD) and differential thermal–thermogravimetric analyses (DTA–TG) were used for characterizing $C\bar{S}A$ cement samples. XRD analysis was performed by a Philips PW1710 apparatus operating between 5° and 60° 2θ (Cu Kα radiation). A Netzsch Tasc 414/3 apparatus, operating between 20 °C and 1000 °C with a heating rate of 10 °C/min, was used to carry out simultaneous DTA–TG analysis.

In addition to the assessment of the clinker mineralogical composition, XRD was employed for detecting reactants and products in cement pastes. Before the test, the pastes (w/s mass ratio, 0.5) were placed in polyethylene bags inside a Haake DC50 thermostatic bath at 20 °C; at the end of curing time, they were removed from the bags and treated with the same procedures used for the porosimetric specimens except for a final step of grinding after which they were obtained in a pulverized form.

The main reaction products, ettringite and aluminium hydroxide, were also identified by DTA–TG analysis; they are formed according to the following reaction of $C_4A_3\bar{S}$ hydration:

$$\underset{(610)}{C_4A_3\bar{S}} + 2\underset{(136)}{C\bar{S}} + 38\underset{(18)}{H} \Rightarrow \underset{(1254)}{C_6A\bar{S}_3H_{32}} + 2\underset{(156)}{AH_3} \quad (1)$$

Table 3
Reactants conversion and products formation in $C\bar{S}A$ cement pastes cured at various aging times—XRD data[a]

		15 m	30 m	1 h	3 h	6 h	1 day	2 days	7 days	14 days	28 days
Reactants	$C_4A_3\bar{S}$	++++	++++	++++	++++	++++	+++	+++	+++	+++	+++
	$C\bar{S}$	++	++	++	++	++	++	++	++	++	++
	α'-C_2S	+	+	+	+	+	+	+	+	+	+
	$C_{12}A_7$	+	+	–	–	–	–	–	–	–	–
Products	$C_6A\bar{S}_3,H_{32}$	+	+	++	+++	+++	++++	++++	++++	++++	++++
	AH_3	–	–	–	+	+	+	+	+	+	+
	$C\bar{S}\cdot 2H_2O$	+	+	–	–	–	–	–	–	–	–

[a] Symbols indicate peak intensities. ++++=very high, +++=high, ++=medium, +=low.

Each figure in parenthesis under the compound formula indicates its molecular weight.

3. Results and discussion

It is well assessed that the peculiar strength development of rapid-hardening $C\bar{S}A$ cements is related to the $C_4A_3\bar{S}$ hydration which is very rapid at early ages and then quickly decreases due to the lack of water: the reaction of $C_4A_3\bar{S}$ with $CaSO_4$ and H_2O for the full formation of ettringite and aluminium hydroxide requires a high stoichiometric water/solid mass ratio, $(w/s)_{st}$. According to Eq. (1), $(w/s)_{st} = \frac{38\cdot 18}{610+2\cdot 136} = 0.78$.

The XRD kinetic data (Table 3 and Fig. 1) clearly show the fast generation of ettringite and the persistence of unhydrated phases at longer curing times. With regard to $C_4A_3\bar{S}$ hydration, the rapid increase of the ettringite concentration, followed by the attainment of a steady-state, can be also observed from the DTA–TG thermograms, shown in Fig. 2, where the DTA endothermal peaks at about 160–170 °C and 270–280 °C are related to ettringite and aluminium hydroxide, respectively.

As far as Portland cement hydration is concerned, the evolution of the porosimetric curves as a function of curing time and water/cement ratio is well established [30–37]. Both increased curing time and decreased w/c ratio give rise to lower values of total porosity and threshold pore width. The differential curves for pastes cured at early ages tend to exhibit a sharply defined initial peak, indicating a unimodal distribution of pore sizes. As curing time increases, a second peak appears at smaller pore sizes thus suggesting a bimodal

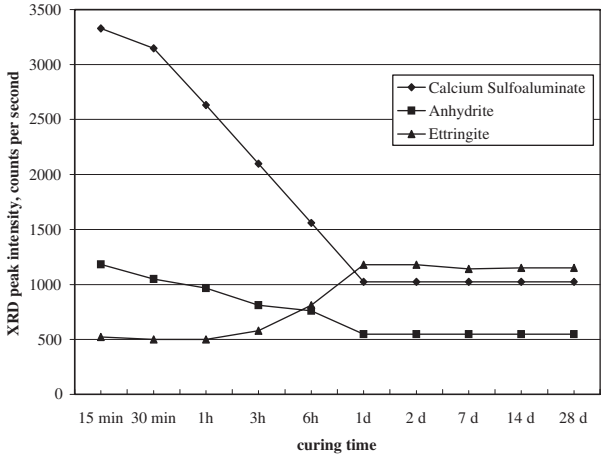

Fig. 1. Net intensity (above the background level) of the main XRD peaks of calcium sulfoaluminate, anhydrite and ettringite in $C\bar{S}A$ cement pastes cured at various ages.

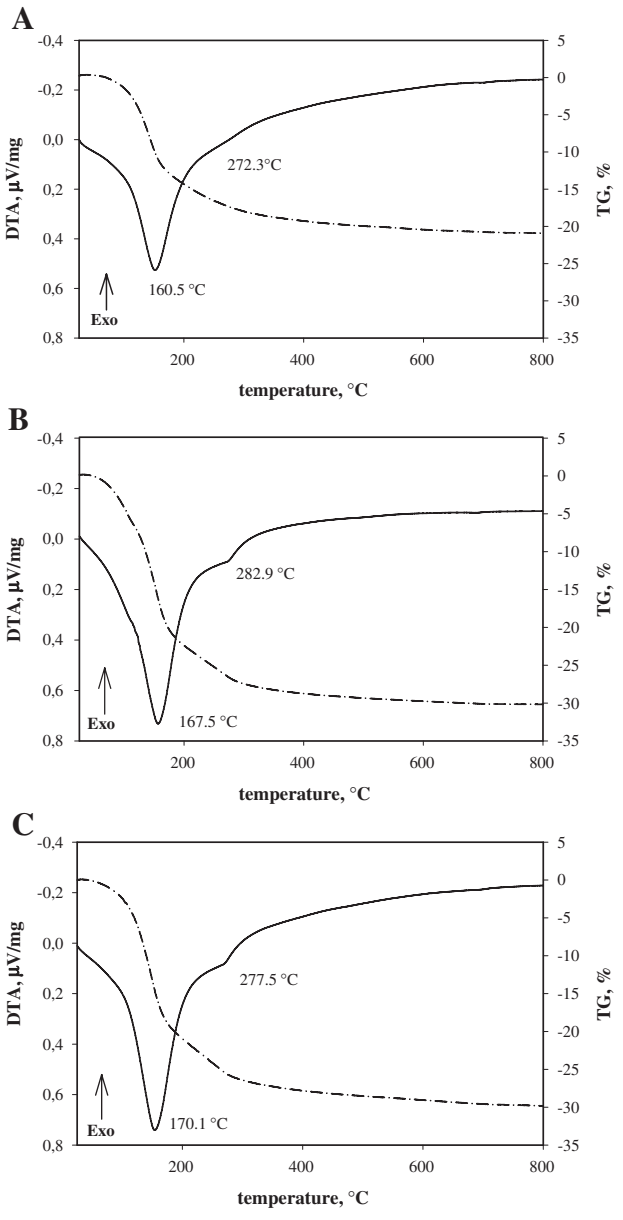

Fig. 2. Thermograms for $C\bar{S}A$ cement pastes cured at 3 h (A), 1 day (B) and 28 days (C). DTA, solid line; TG, dotted line.

distribution. The first peak is related to the lowest size of pore necks connecting a continuous system. The second peak seems to correspond to the pressure required to break through the blockages formed by the hydration products which isolate the interior pore space.

According to widespread opinion [36,37], mercury intrusion porosimetry plots do not represent the actual distribution of pore sizes in hydrated cementitious systems. Large internal pores mostly open only to smaller pores communicating with the outside. They cannot fill until the higher pressures are reached that are needed for the mercury penetration into the smaller pores. Therefore, almost all the volume of larger pores is mistakenly allocated to the size of the smaller ones. Moreover, the measured intrudable porosity does not coincide with the total porosity because, in addition to the pore space actually intruded by mercury, finer pores are present in cement pastes that require a pressure value for entry higher than the maximum available pressure of the commercial instrumentation. A few isolated pores that are entirely sealed against intrusion may exist as well. However, for comparative evaluations like those performed in this investigation, the threshold pore radius and the total volume of intruded mercury can be taken as useful indicators of the process of space filling and of pore refinement.

Fig. 3 illustrates the porosimetric curves for the pastes of both investigated cements. Fig. 3A and B show, respectively, cumulative and derivative Hg volume for Portland cement pastes cured at 12 h, 1 day, 7 days and 28 days. As expected, the distribution of pore sizes is unimodal at earlier ages while it is bimodal at longer periods. As curing time increases, both cumulative Hg volume and first threshold pore radius decrease from 169 to 79 mm^3/g and from 650 to about 350 nm, respectively. The second threshold pore radius is roughly included within the range 10–30 nm.

Fig. 3C and D show, respectively, cumulative and derivative Hg volume for $C\bar{S}A$ cement pastes cured at 2 h, 6 h, 12 h, 1 day, 7 days and 28 days. It can be noted that a bimodal distribution rapidly occurs. After 2 h of aging the lower porosity region contributes about 25% of the total intruded volume while at longer curing times the role of the smaller pores becomes dominant. Within the first 12 h of hydration, the cumulative Hg volume and the first threshold pore radius decrease from 119 to

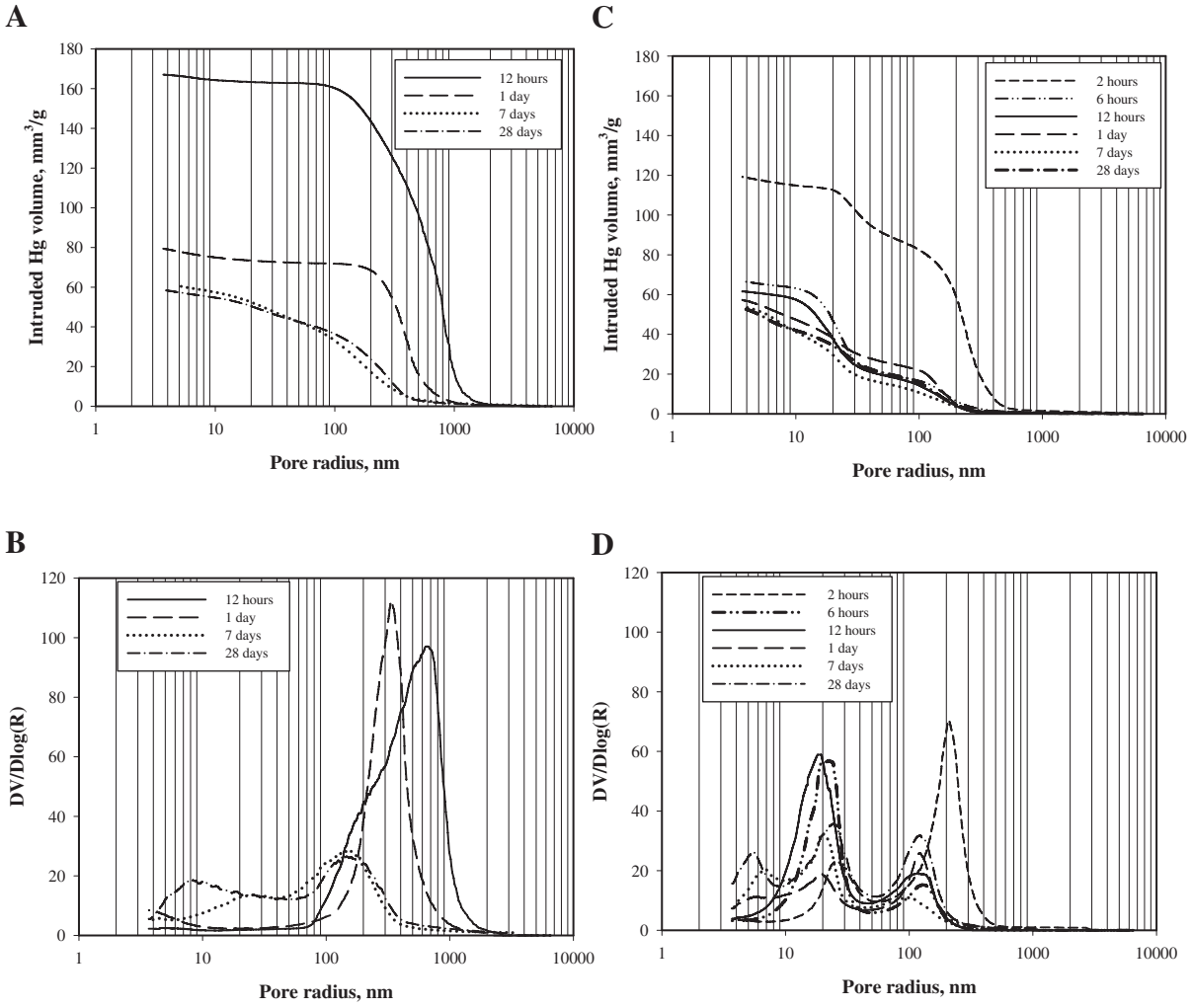

Fig. 3. Intruded Hg volume vs. pore radius for cement pastes cured at various ages: (A) Portland cement, cumulative plot; (B) Portland cement, derivative plot; (C) sulfoaluminate cement, cumulative plot; (D) sulfoaluminate cement, derivative plot.

61 mm^3/g and from 200 to about 150 nm, respectively; the second threshold pore radius is about 20–25 nm.

According to the characteristics of the $C\overline{S}A$ cement hydration pointed out by XRD, DTA, and TG analyses, the development of the pore structure is initially very fast and a prevailing region of lower porosity is established because sufficient hydration products are rapidly formed to reduce and isolate the interior space. At longer curing times, the evolution of porosity proceeds very slowly because hydration is almost stopped.

The comparison between the results obtained with Portland and $C\overline{S}A$ cement pastes at 12 h of aging clearly shows the strong difference in the porosimetric characteristics. The evolution of porosity for $C\overline{S}A$ cement pastes cured in the period of 1–28-days is also completely different from that observed for Portland cement pastes, even if at 7 and 28 days of aging total intruded volume, first and second threshold pore radius do not vary significantly. It is interesting to note the appearance of a trimodal distribution inasmuch as the lower porosity field is split in two regions with two threshold pore radii ranging from 20 to 25 nm and from 5.5. to 7 nm.

4. Conclusions

A rapid-hardening calcium sulfoaluminate cement, when paste hydrated at early ages, shows porosimetric characteristics completely different from those of a Portland cement. The very fast reaction rate of calcium sulfoaluminate consumes the mix water in a short time so as to stop at later ages the evolution of total porosity. The hydration products, quickly generated in a large amount at earlier curing times, are able to decrease and refine the interior pore space. Hence, a bimodal distribution of pore sizes is achieved quickly, in which , except at the shortest aging time (2 h), the regions of smaller pores (having a threshold pore radius up to 25 nm) prevail over that related to an interconnected capillary network (with a threshold pore radius up to 200 nm).

For Portland cement pastes, on the contrary, a continuous pore network (with a threshold pore radius between about 350 and 650 nm) solely contributes at early ages (up to 1 day) to total porosity (unimodal distribution). Only at longer ages discontinuous regions of lower porosity appear, due to the blockages of the hydration products (bimodal distribution).

The special evolution of porosity in hydrated calcium sulfoaluminate cements undoubtedly has a very important role in promoting their better performance in terms of early strength, impermeability, chemical resistance and other engineering properties.

Acknowledgements

The authors wish to express their gratitude to Prof. F.P. Glasser for his valuable suggestions.

References

[1] Klein Symposium on Expansive Cement Concretes, ACI Publication SP-38, Detroit, USA, 1973.
[2] W. Kurdowski, Expansive cements, Proc. 7th Int. Congr. Chem. Cem., Paris, France, 1980, vol. I, pp. V-2/1–V-2/10.
[3] W. Kurdowski, C.M. George, F.P. Sorrentino, Special cements, Proc. 8th Int. Congr. Chem. Cem., Rio de Janeiro, Brasil, 1986, vol. I, pp. 293–318.
[4] Su Muzhen, W. Kurdowski, F.P. Sorrentino, Development in non-Portland cements, Proc. 9th Int. Congr. Chem. Cem., New Delhi, India, 1992, vol. I, pp. 317–356.
[5] T.V. Kouznetsova, Development of special cements, Proc. 10th Int. Congr. Chem. Cem., Goteborg, Sweden, 1997, vol. 1, p. 1i001, 4 pp.
[6] K.L. Scrivener, Properties, applications and practicalities of special cements, Proc. 11th Int. Congr. Chem. Cem., Durban, South Africa, 2003, vol. 1, pp. 84–93.
[7] P.K. Mehta, Investigations on energy-saving cements, World Cem. Technol. 11 (4) (1980) 166–177.
[8] G.A. Mudbhatkal, P.S. Parmeswaran, A.S. Heble, B.V.B. Pai, A.K. Chatterjee, Non-alitic cement from calcium sulphoaluminate clinker—optimisation for high-strength and low-temperature application, Proc. 8th Int. Congr. Chem. Cem., Rio de Janeiro, Brazil, 1986, vol. IV, pp. 364–370.
[9] J. Beretka, L. Santoro, N. Sherman, G.L. Valenti, Synthesis and properties of low energy cements based on $C_4A_3\overline{S}$, Proc. 9th Int. Congr. Chem. Cem., New Delhi, India, 1992, vol. III, pp. 195–200.
[10] J. Beretka, B. de Vito, L. Santoro, N. Sherman, G.L. Valenti, Hydraulic behaviour of calcium sulphoaluminate-based cements derived from industrial process wastes, Cem. Concr. Res. 23 (1993) 1205–1214.
[11] J. Majling, S. Sahu, M. Vlna, Della M. Roy, Relationship between raw mixture and mineralogical composition of sulphoaluminate belite clinkers in the system $CaO\text{-}SiO_2\text{-}Al_2O_3\text{-}Fe_2O_3\text{-}SO_3$, Cem. Concr. Res. 23 (1993) 1351–1356.
[12] G. Belz, J. Beretka, M. Marroccoli, L. Santoro, N. Sherman, G.L. Valenti, Use of fly ash, blast furnace slag and chemical gypsum for the synthesis of calcium sulphoaluminate based cements, Proc. 5th CANMET/ACI Int. Conf. on Fly Ash, Silica Fume, Slag and Natural Pozzolans in Concrete, Milwaukee, USA, 1995, SP-153, 1995, vol. 1, pp. 513–530.
[13] J. Beretka, R. Cioffi, M. Marroccoli, G.L. Valenti, Energy-saving cements obtained from chemical gypsum and other industrial wastes, Waste Manage. 16 (1996) 231–235.
[14] K. Ikeda, K. Fukuda, H. Shima, Calcium sulphoaluminate cements prepared from low-alumina waterworks slime, Proc. 10th Int. Congr. Chem. Cem., Goteborg, Sweden, 1997, vol. 1, pp. 1i025, 8 pp.
[15] P. Arjunan, M.R. Silsbee, Della M. Roy, Sulfoaluminate-belite cement from low-calcium fly ash and sulphur-rich and other industrial by-products, Cem. Concr. Res. 29 (1999) 1305–1311.
[16] G. Bernardo, M. Marroccoli, F. Montagnaro, G.L. Valenti, Use of fluidized bed combustion wastes for the synthesis of low energy cements, Proc. 11th Int. Congr. Chem. Cem., Durban, South Africa, 2003, vol. 3, pp. 1227–1236.
[17] Deng Jun-An, Ge Wen-Min, Su Mu-zhen, Li Xiu-Ying, Sulfoaluminate cement series, Proc. 7th Int. Congr. Chem. Cem., Paris, France, 1980, vol. IV, pp. 381–386.
[18] Wang Yanmou, Su Muzhen, The third series cement in China, Proceedings of the Third International Symposium on the Cement and Concrete, Shanghai, China, 1993, vol. 3, pp. 116–121.
[19] Muzhen Su, Yanmou Wang, Liang Zhang, Dedong Li, Preliminary study on the durability of sulfo/ferro-aluminate cements", Proc. 10th Int. Congr. Chem. Cem., Goteborg, Sweden, 1997, vol. 4, pp. 4iv029, 12 pp.
[20] Tangbo Sui, Yan Yao, Recent progress in special cements in China, Proc. 11th Int. Congr. Chem. Cem., Durban, South Africa, 2003, vol. 4, pp. 2028–2032.
[21] J. Pera, J. Ambroise, New applications of calcium sulphoaluminate cement, Cem. Concr. Res. 34 (2003) 671–676.
[22] J. Pera, J. Ambroise, M. Chabannet, Valorization of automotive shredder residue in building materials, Cem. Concr. Res. 34 (2004) 557–562.
[23] Wang Lan, F.P. Glasser, Hydration of calcium sulphoaluminate cements, Adv. Cem. Res. 8 (31) (1996) 127–134.
[24] L. Zhang, F.P. Glasser, New concretes based on calcium sulphoaluminate cements, in: R.K. Dhir, D. Dyer (Eds.), Modern Concrete Materials, Thomas Telford, London, 1999, pp. 261–274.

[25] F.P. Glasser, L. Zhang, High-performance cement matrices based on calcium sulphoaluminate-belite compositions, Cem. Concr. Res. 31 (2001) 1881–1886.
[26] F.P. Glasser, Advances in sulphoaluminate cements, Proceedings of the 5th International Symposium on the Cement and Concrete, Shanghai, China, 2002, vol. 1, pp. 14–24.
[27] J. Beretka, M. Marroccoli, N. Sherman, G.L. Valenti, The influence of $C_4A_3\overline{S}$ content and w/s ratio on the performance of calcium sulphoaluminate-based cements, Cem. Concr. Res. 26 (11) (1996) 1673–1681.
[28] F.P. Glasser, L. Zhang, Calculation of chemical water demand for hydration of calcium sulphoaluminate cement, Proceedings of the 4th International Symposium on the Cement and Concrete, Shanghai, China, 1998, vol. 3, pp. 38–44.
[29] D.N. Winslow, S. Diamond, A mercury porosimetry study of the evolution of porosity in Portland cement, ASTM J. Mater. 3 (1970) 564–585.
[30] A. Bentur, The pore structure of hydrated cementitious compounds of different chemical composition, J. Am. Ceram. Soc. 63 (7–8) (1980) 381–386.
[31] Ö.Z. Cebeci, Pore structure of air-entrained hardened cement paste, Cem. Concr. Res. 11 (1981) 257–265.
[32] H.G. Midgley, J.M. Illston, Some comments on the microstructure of hardened cement pastes, Cem. Concr. Res. 13 (1983) 197–206.
[33] I. Odler, M. Rößler, Investigations on the relationship between porosity, structure, and strength of hydrated Portland cement pastes: II. Effect of pore structure and of degree of hydration, Cem. Concr. Res. 15 (1985) 401–410.
[34] E.J. Garboczi, Permeability, diffusivity, and microstructural parameters: a critical review, Cem. Concr. Res. 20 (1990) 591–601.
[35] N. Hearn, R.D. Hooton, Sample mass and dimension effects on mercury intrusion porosimetry results, Cem. Concr. Res. 22 (5) (1992) 970–980.
[36] R.A. Cook, K.C. Hover, Mercury porosimetry of hardened cement pastes, Cem. Concr. Res. 29 (1999) 933–943.
[37] S. Diamond, Mercury porosimetry–an inappropriate method for the measurement of pore size distributions in cement-based materials, Cem. Concr. Res. 30 (2000) 1517–1525.